Genetic Analysis of Endocytosis in *Caenorhabditis elegans*: Coelomocyte Uptake Defective Mutants

Hanna Fares*,† and Iva Greenwald*

**Department of Biochemistry and Molecular Biophysics, Howard Hughes Medical Institute, Columbia University College of Physicians and Surgeons, New York, New York 10032 and †Department of Molecular and Cellular Biology, University of Arizona, Tucson, Arizona 85721*

Manuscript received May 1, 2001
Accepted for publication May 25, 2001

ABSTRACT

The coelomocytes of *Caenorhabditis elegans* are scavenger cells that continuously and nonspecifically endocytose fluid from the pseudocoelom (body cavity). Green fluorescent protein (GFP) secreted into the pseudocoelom from body wall muscle cells is endocytosed and degraded by coelomocytes. We show that toxin-mediated ablation of coelomocytes results in viable animals that fail to endocytose pseudocoelomic GFP, indicating that endocytosis by coelomocytes is not essential for growth or survival of *C. elegans* under normal laboratory conditions. We examined known viable endocytosis mutants, and performed RNAi for other known endocytosis genes, for *c*oelomocyte *up*take defective (Cup) phenotypes. We also screened for new genes involved in endocytosis by isolating viable mutants with Cup defects; this screen identified 14 different genes, many with multiple alleles. A variety of Cup terminal phenotypes were observed, consistent with defects at various steps in the endocytic pathway. Available molecular information indicates that the Cup mutant screen has identified novel components of the endocytosis machinery that are conserved in mammals but not in *Saccharomyces cerevisiae*, the only other organism for which large-scale genetic screens for endocytosis mutants have been performed.

ENDOCYTOSIS is a basic function of eukaryotic cells that leads to the internalization of fluid from the extracellular medium, nutrient uptake, and the recycling of membrane components. In multicellular organisms, endocytosis has also been adapted by specialized cells for specific functions, including the downregulation of signaling, synaptic vesicle recycling, and antigen presentation. There are various routes by which endocytosis is accomplished, involving different cellular structures: clathrin-coated pits, non-clathrin-coated pits, caveolae, and macropinosomes (Watts and Marsh 1992; Robinson *et al.* 1996; Mukherjee *et al.* 1997). The particular mechanism used to regulate these pathways depends on the ligand being internalized and the cell type examined. The multiplicity of options adds complexities that suggest that endocytosis should be studied using several different approaches and experimental systems.

Many of the steps in endocytosis have been determined through studies on mammalian tissue culture cells that are technically suited for this kind of analysis (Watts and Marsh 1992; Robinson *et al.* 1996; Mukherjee *et al.* 1997). In brief, a vesicle containing the internalized medium buds from the membrane. The internalized substances then are sorted as they traverse a series of membranous compartments, called endosomes, before either reaching the lysosomes to be degraded or getting recycled to the surface. Many different protein components of these vesicles have been identified through biochemical methods using mammalian cell culture systems.

Genetic analysis has also been an important tool for dissecting endocytosis. The most extensive and informative screens have been done in the yeast *Saccharomyces cerevisiae* (Riezman 1985; Chvatchko *et al.* 1986; Munn and Riezman 1994; Wendland *et al.* 1996; Zheng *et al.* 1998). For example, numerous insights into the machinery involved in the trafficking of molecules between the Golgi compartment, endosomes, and the vacuole (yeast lysosome) have emerged from such investigations (Lemmon and Traub 2000). In particular, these studies have been crucial in elucidating protein complexes involved in the retrograde transport of molecules to the Golgi compartment.

Multicellular organisms utilize endocytosis in many more contexts than do unicellular organisms, raising the possibility that they exhibit differences in regulating endocytosis. One such difference between yeast cells and mammalian cells, for example, is that the adaptor complexes are not needed for clathrin function or for endocytosis in yeast (Huang *et al.* 1999; Yeung *et al.* 1999). Although screens for mutants defective in endocytosis have been carried out in mammalian cells (Robbins *et al.* 1983; Krieger 1986; Colbaugh *et al.* 1988; Hobbie *et al.* 1994) and in *Dictyostelium discoideum* (Bacon *et al.* 1994), the only concerted effort to screen for endocytosis mutants in a multicellular organism has been the study of the receptor-mediated endocytosis of yolk in *Caenorhabditis elegans* oocytes (Grant and Hirsh

Corresponding author: Hanna Fares, University of Arizona, Department of Molecular and Cellular Biology, Life Sciences South Bldg., Rm. 531, 1007 E. Lowell St., Tucson, AZ 85721.
E-mail: fares@email.arizona.edu

1999). *C. elegans* is particularly suited to large-scale genetic screens, and many genes that are conserved in worms and humans are not found in yeast (Lander *et al.* 2001; Venter *et al.* 2001). Indeed, the molecular analysis of *C. elegans* endocytosis mutants so far has demonstrated that novel components involved in endocytosis unique to multicellular organisms can be identified using genetic analysis in *C. elegans* (see discussion).

Here, we report an approach to studying endocytic pathways in *C. elegans*, using an assay based on the uptake of fluid-phase markers from the pseudocoelom by coelomocytes. We show that in this *c*oelomocyte *up*take (Cup) assay many different fluid-phase markers can be endocytosed by coelomocytes. We describe the behavior of known endocytosis mutants and RNA-mediated interference (RNAi) for known endocytosis genes using the Cup assay and the results of a screen for viable *cup* mutants. This work establishes the Cup assay as a powerful genetic screen for endocytosis mutants in a multicellular organism.

MATERIALS AND METHODS

***C. elegans* methods and strains:** General methods for the handling and maintenance of *C. elegans* are as described previously (Brenner 1974). The wild-type parent for all strains was *C. elegans* var. Bristol (Brenner 1974), except for sequence-tagged site (STS) mapping that used var. Bergerac strain DP13 (Williams *et al.* 1992). Standard methods were used for genetic analysis (Brenner 1974), DNA microinjection (Fire 1986; Mello *et al.* 1991), and double-stranded RNA synthesis and microinjection (Fire *et al.* 1998).

Plasmid construction: pJF25 [p*myo-3::ssGFP*] (Fares and Greenwald 2001) has DNA encoding the first 79 amino acids from SEL-1 (Grant and Greenwald 1997), including a signal sequence, fused to green fluorescent protein (GFP; Chalfie *et al.* 1994), with the S65T substitution, and under the control of the *myo-3* promoter.

pJF43 [p*hsp::ssGFP*] (Fares and Greenwald 2001) has DNA encoding the SEL-1 (Grant and Greenwald 1997) signal sequence-GFP fusion under the control of the *hsp16-41* (Jones *et al.* 1986) heat-shock promoter.

To make a construct expressing the Diphtheria toxin A fragment (catalytic) specifically in coelomocytes, we used plasmid pcc1 (P. Sengupta, personal communication), which was made by subcloning a 3993-bp fragment, now known to be the upstream region of *unc-122* (P. Loria and O. Hobert, personal communication), into plasmid pPD95.77 (A. Fire, personal communication). pcc1 therefore has a GFP coding sequence with *unc-122* 5′ sequences upstream and *unc-54* 3′-untranslated sequences downstream. When transformed into worms, GFP is almost exclusively seen in coelomocytes, albeit in a few worms, one or more coelomocytes are not fluorescent or are more weakly fluorescent. In addition, very occasional weak expression is also seen in certain neurons.

We used the polymerase chain reaction (PCR) to amplify a 0.6-kb fragment from plasmid pDT-AK51E (DeLange *et al.* 1979) using the primers J197 (CACACAGGATCCAAAATGG GCGCTGATGATGTTGTTGATTC; *Bam*HI site is underlined) and J198 (CACACAGAATTCTCATTAACGATTTCCTGCACA GGC; *Eco*RI site is underlined). The amplified PCR fragment was restriction digested with *Bam*HI and *Eco*RI and subcloned into the same sites in pcc1. The resulting plasmid, pJF142, has the Diptheria toxin A fragment bearing a K51E substitution replacing GFP in plasmid pcc1. The Diptheria toxin A fragment bearing a K51E substitution has 10% of the activity of the wild-type protein (DeLange *et al.* 1979).

Transgenes and strains: Extrachromosomal arrays were generated by coinjecting plasmid DNA at 1–50 μg/ml along with the marker plasmids pRF4 [*rol-6(su1006)*] (Mello *et al.* 1991) or pMH86 [*dpy-20(+)*] (Han and Sternberg 1991) into the germline and were integrated by irradiation using standard methods (Mello and Fire 1995).

*arIs37[*p*myo-3::ssGFP]* (Fares and Greenwald 2001) was made by integrating an extrachromosomal array that was made by injecting a DNA mix containing pJF25 [p*myo-3::ssGFP*] (62.5 μg/ml) + pMH86 (20 μg/ml) + pBluescript SK$^+$ (100 μg/ml; Stratagene, La Jolla, CA) in a *dpy-20(e1282)* (Hosono *et al.* 1982) background. The isolated integrant was backcrossed eight times to *dpy-20(e1282)* prior to use. We checked 107 Unc F_1 progeny segregating from *dpy-20(e1282); arIs37[*p*myo-3::ssGFP]/ unc-54(e190)* hermaphrodites: all were Dpy, suggesting that *arIs37[*p*myo-3::ssGFP]* maps close to *unc-54(e190)* on chromosome I. However, we were eventually able to construct an *unc-54(e190) arIs37[*p*myo-3::ssGFP]* strain.

*arIs36[*p*hsp::ssGFP]* (Fares and Greenwald 2001) was made by integrating an extrachromosomal array that was made by injecting a DNA mix containing pJF43 [p*hsp::ssGFP*] (20 μg/ml) + pMH86 (25 μg/ml) + pBluescript SK$^+$ (100 μg/ml) in a *dpy-20(e1282)* background. The integrant was backcrossed twice to *dpy-20(e1282)* prior to use.

*arEx218[*p*cc1::DT-A$_{K51E}$]* was made by injecting a DNA mix containing pJF142 [p*cc1::DT-A$_{K51E}$*] (10 μg/ml) + pRF4 (100 μg/ml) into *dpy-20(e1282); arIs37[*p*myo-3::ssGFP]* hermaphrodites.

All other genetic markers used in this article can be found referenced in the *C. elegans II* book by Riddle *et al.* (1997), except for *eat-20(nc4)* (Shibata *et al.* 2000), *nrf-4(sa528)*, *nrf-5(sa513)*, and *nrf-6(sa525)* (Choy and Thomas 1999), and *spg-(e2335)* (L. Avery, personal communication).

Molecular analysis: Standard methods were used for the manipulation of recombinant DNA (Sambrook *et al.* 1989). All enzymes were from New England Biolabs (Beverly, MA), unless otherwise indicated. PCR was done using the Expand Long Template PCR system (Boehringer Mannheim, Mannheim, Germany) according to the manufacturer's instructions.

Mutant screen and mapping: Adult *dpy-20(e1282); arIs37 [*p*myo-3::ssGFP]* hermaphrodites were mutagenized using ethyl methanesulfonate (EMS) as previously described (Brenner 1974). Five mutagenized parents were placed on a single nematode growth media (NGM; Brenner 1974) plate that had been previously seeded with *Escherichia coli* OP50 (Brenner 1974). The F_2 hermaphrodites from each plate were screened for a defect in endocytosis by coelomocytes (evidenced by a change in the amount of GFP in the pseudocoelom and/or coelomocytes) using a modified dissection microscope equipped with fluorescence optics (Zeis, Thornwood, NY). Mutant F_2 worms were picked onto individual fresh NGM plates (with OP50).

We mutagenized 720 P_0 hermaphrodites and checked the progeny from ~18,000 F_1 hermaphrodites. We picked 175 adult F_2 mutant hermaphrodites (not independent isolates) of which 97 did not give viable progeny. To ensure independent isolation of mutants, we chose only one mutant from each plate, except for two cases in which the mutant phenotypes were distinguishably different; in both cases, the two mutants picked from the same plate had mutations that mapped to different locations (see below). We also saw many F_2 hermaphrodites that had strong accumulations of GFP in the pseudocoelom but that were arrested at earlier larval stages; these were neither counted nor picked to separate plates. Finally, we kept 55 viable mutant hermaphrodites for further analysis.

We first backcrossed the 55 mutant hermaphrodites three times to *dpy-20(e1282); arIs37[*p*myo-3::ssGFP]* males. We then mapped the backcrossed mutations to a region of the genome using STS mapping, as previously described (Williams *et al.* 1992). Individual *cup* mutations were tested by complementation analysis for the Cup phenotype against all *cup* and *rme* mutations that mapped to the same region and against some other mutations (see below) in the same region. We thus determined that the 55 mutations defined 14 genes. Three of these, *rme-1*, *rme-6*, and *rme-8*, were previously identified as mutants defective in yolk uptake by oocytes (Grant and Hirsh 1999). We named the rest *cup-1* through *cup-11* (*cup* is the *c*oelomocyte *up*take defect); these were mapped further using conventional markers.

cup-1 I: We isolated 48 recombinants from *unc-101(m1) glp-4(bn2) arIs37[*p*myo-3::ssGFP]/cup-1(ar478) arIs37[*p*myo-3::ssGFP]* hermaphrodites. Of the 48 Unc non-Glp recombinants, 31 picked up *cup-1(ar478)*. *cup-1(ar478)* complemented *nrf-4(sa528)*.

cup-2 I: We isolated 55 recombinants from *dpy-24(s71) unc-101(m1) arIs37[*p*myo-3::ssGFP]/cup-2(ar506) arIs37[*p*myo-3::ssGFP]* hermaphrodites. None of the 23 Dpy non-Unc recombinants picked up *cup-2(ar506)*. All of the 32 Unc non-Dpy recombinants picked up *cup-2(ar506)*. We also isolated 36 recombinants from *unc-13(e51) dpy-24(s71) arIs37[*p*myo-3::ssGFP]/cup-2(ar506) arIs37[*p*myo-3::ssGFP]* hermaphrodites. None of the 36 Dpy non-Unc recombinants picked up *cup-2(ar506)*. Thus, *cup-2(ar506)* maps close to *dpy-24(s71)*. *cup-2(ar506)* complemented *nrf-4(sa528)* and *dyf-5(mn400)*.

cup-3 II: We isolated 38 recombinants from *dpy-10(e128) unc-4(e120)/cup-3(ar496); arIs37[*p*myo-3::ssGFP]* hermaphrodites. Of the 15 Dpy non-Unc recombinants, 5 picked up *cup-3(ar496)*. Of the 23 Unc non-Dpy recombinants, 10 picked up *cup-3(ar496)*. *cup-3(ar496)* complemented *nrf-6(sa525)* and *dyf-13(mn396)*.

cup-4 III: We isolated 10 recombinants from *sma-3(e491) unc-36(e251)/cup-4(ar494); arIs37[*p*myo-3::ssGFP]* hermaphrodites. Of the 6 Sma non-Unc recombinants, 4 picked up *cup-4(ar494)*. Of the 4 Unc non-Sma recombinants, 1 picked up *cup-4(ar494)*.

cup-5 III: We isolated 18 recombinants from *sma-3(e491) unc-36(e251)/cup-5(ar465); arIs37[*p*myo-3::ssGFP]* hermaphrodites. Of the 10 Sma non-Unc recombinants, 5 picked up *cup-5 (ar465)*. Of the 8 Unc non-Sma recombinants, 5 picked up *cup-5(ar465)*.

cup-6 III: We isolated 23 recombinants from *unc-25(e156) bli-5(e518)/cup-6(ar513); arIs37[*p*myo-3::ssGFP]* hermaphrodites. Of the 20 Unc non-Bli recombinants, 19 picked up *cup-6 (ar513)*. None of the 3 Bli non-Unc recombinants picked up *cup-6(ar513)*. We also isolated 71 recombinants from *dpy-18 (e364) unc-64(e246)/cup-6(ar513); arIs37[*p*myo-3::ssGFP]* hermaphrodites. Of the 36 Dpy non-Unc recombinants, 35 picked up *cup-6(ar513)*. None of the 35 Unc non-Dpy recombinants picked up *cup-6(ar513)*. Thus, while *cup-6* maps to the extreme right arm of chromosome III, due to the single recombinant from each mapping cross, we cannot confirm its exact location relative to the markers used. *cup-6(ar513)* complemented *dyf-2(m160)*.

cup-7 IV: We isolated 15 recombinants from *lin-1(e1275) unc-33(e204)/cup-7(ar492); arIs37[*p*myo-3::ssGFP]* hermaphrodites. Of the 15 Lin non-Unc recombinants, 6 picked up *cup-7 (ar492)*. *cup-7(ar492)* complemented *unc-17(e245)*, *dpy-13(e184)*, *dpy-9(e2)*, *ced-2(e1752)*, *unc-33(e204)*, *cha-1(p1152)*, *eat-7(ad450)*, *eat-10(ad606)*, and *dyf-3(m185)*.

cup-8 V: We isolated three recombinants from *unc-34(e566) unc-60(e677) dpy-11(e224)/cup-8(ar466); arIs37[*p*myo-3::ssGFP]* hermaphrodites. All three Unc-34 non-Unc-60 recombinants picked up *cup-8(ar466)*. We then picked 252 F_1 Unc-34 hermaphrodites from *unc-34(e566) cup-8(ar466)/unc-60(e723); arIs37[*p*myo-3::ssGFP]* hermaphrodites. Four of these were recombinants between *unc-34(e566)* and *unc-60(e723)*. Two of these recombinants also picked up *cup-8(ar466)*. *cup-8(ar466)* complemented *nrf-5(sa513)*.

cup-9 V: We isolated 22 recombinants from *sma-1(e30) unc-39(e257)/cup-9(ar467); arIs37[*p*myo-3::ssGFP]* hermaphrodites. Of the 14 Sma non-Unc recombinants, 6 picked up *cup-9 (ar467)*. Of the 8 Unc non-Sma recombinants, 5 picked up *cup-9(ar467)*. *cup-9(ar467)* complemented *nrf-5(sa513)* and *dyf-4(m158)*.

cup-10 V: We isolated 47 Dpy non-Lag recombinants from *lag-2(q420) dpy-11(e224)/cup-10(ar479); arIs37[*p*myo-3::ssGFP]* hermaphrodites: 4 picked up *cup-10(ar479)*. We tested whether *cup-10(ar479)* could complement deletions in that region (D. Baillie, personal communication). *cup-10(ar479)* did not complement the deficiencies *sDf26*, *sDf28*, *sDf42*, and *sDf50*. *cup-10(ar479)* did complement *sDf31*, *sDf32*, *sDf45*, and *sDf46*. *cup-10(ar479)* complemented *nrf-5(sa513)*.

cup-11 X: We isolated 15 Unc non-Mup recombinants from *mup-2(e2346) unc-6(e78)/cup-11(ar472); arIs37[*p*myo-3::ssGFP]* hermaphrodites: 9 picked up *cup-11(ar472)*. *cup-11(ar472)* complemented *dyn-1(ky51ts)*.

Phenotypic analysis of mutants: To check for defects in yolk uptake by the oocytes, the backcrossed mutant strains and their unmutagenized parent strain were grown on NGM (+OP50) plates at 20° and gravid adult hermaphrodites were checked by Nomarski microscopy for the accumulation of lipid droplets in the pseudocoelom. This test may not be sensitive enough to score mutants that have only a mild defect in oocyte uptake.

To check for defects in the uptake of substances by intestinal cells from the lumen of the gut, we placed three L4 of the backcrossed mutant strains and their wild-type parent on individual NGM (+OP50; no cholesterol) plates at 20°; these NGM plates did not have any added cholesterol and also contained rhodamine-conjugated dextran (M_r 11,000) added at 0.1 mg/ml. Adult F_1 hermaphrodites were visually checked by fluorescence microscopy for the uptake of the rhodamine-conjugated dextran by the intestinal cells. The two mutants that did show a defect were retested on regular NGM plates (+OP50) that were not lacking in cholesterol but still had the rhodamine-conjugated dextran.

Injections into the pseudocoelom: Substances were injected into the pseudocoelom of 7–10 adult *dpy-20(e1282); arIs37 [*p*myo-3:ssGFP]* hermaphrodites and kept at 20° on NGM (+OP50) plates. The injected worms were then checked at various times up to 24 hr.

Chemicals: All chemicals used in this research were purchased from Sigma (St. Louis), except for Lucifer Yellow, Bodipy-conjugated cholesterol, and Transferrin Red, which were purchased from Molecular Probes (Eugene, OR).

Heat-shock experiment: Hermaphrodites grown at 20° were synchronized by collecting the eggs after bleaching and allowing them to hatch on NGM plates. The starved L1 larvae were put on NGM (+OP50) plates and incubated at 20° for 2 more days until the worms were at the L4 stage. The L4 larvae were then heat-shocked at 33° for 30 min before being returned to 20° and checked at different times.

Microscopy: Worms were mounted on a 2% agarose pad in 3.5 μl of 1% formaldehyde. Compound microscope images were taken on a Zeiss (Thornwood, NY) Axioplan.

RESULTS

Coelomocytes endocytose fluid from the pseudocoelom: There are six coelomocytes in the pseudocoelom of adult hermaphrodites; four are present at hatching, and two are generated in the first larval stage

(Chitwood and Chitwood 1974). The coelomocytes are full of membrane-bound compartments of different sizes that can be visualized in the light microscope (Figure 1D). By electron microscopy, the membranes of the coelomocytes appear to have multiple invaginations indicating that they are actively internalizing fluid from the pseudocoelom (White 1988; D. Hall, personal communication). Indeed, GFP secreted into the pseudocoelom from many tissues is taken up predominantly by coelomocytes (Fitzgerald and Greenwald 1995; Grant and Greenwald 1997; Fares and Greenwald 2001; A. Fire, personal communication). We made transgenic worms in which GFP is secreted into the pseudocoelom when it is attached to a signal sequence and expressed in body wall muscles. The GFP is endocytosed and subsequently degraded, primarily by the coelomocytes. Such *arIs37[*p*myo-3::ssGFP]* worms (materials and methods) display diffuse fluorescence in the pseudocoelom and bright fluorescent vesicles in coelomocytes (Figure 1, A–D).

To assay whether there is any specificity in uptake by coelomocytes, we injected various substances into the pseudocoelom. Many different substances proved to be endocytosed efficiently by coelomocytes when injected into the pseudocoelom: india ink (White 1988; J. Kimble, personal communication), rhodamine-dextran (M_r 40,000; C. Winter and D. Hirsh, personal communication), fluorescein isothiocyanate (FITC)-BSA (M_r 71,000), FITC-lipopolysaccharide (LPS) from *Salmonella typhimurium*, FITC-dextran (M_r 35,600), Transferrin Red (M_r 80,500), FITC (M_r 389.4), and rhodamine (M_r 536.1) (Figure 1, E and F; data not shown).

We found two substances that were not efficiently endocytosed [FITC-LPS from *E. coli* and Lucifer Yellow (M_r 521.56)] and two other substances [Bodipy-cholesterol and FITC-conjugated dextran (M_r 2,000,000)] that appeared to be completely excluded. Three of these substances, FITC-LPS (*E. coli*), Bodipy-cholesterol, and Lucifer Yellow, may not be available for uptake because they appear to adhere to yolk granules (Bossinger and Schierenberg 1996; Matyash *et al.* 2001), which are rarely taken up by the coelomocytes (D. Hall, personal communication). However, the failure of FITC-conjugated dextran (M_r 2,000,000) to be taken up by coelomocytes suggests that the coelomocytes nonspecifically endocytose soluble material below a certain size from the pseudocoelom, as FITC-dextran of M_r 35,600 is efficiently endocytosed.

Fate of GFP endocytosed by coelomocytes: To determine the fate of GFP secreted into the pseudocoelom, we did an *in vivo* pulse chase using a strain carrying a transgene that expresses ssGFP from a heat-shock promoter (p*hsp::ssGFP*). GFP is not produced at the normal growth temperature of 20°, but a brief heat shock at 33° results in a finite pulse of GFP secreted into the pseudocoelom. The fate of the GFP can then be followed as a function of time by returning the worms to 20° (Figure 2). We found that, after the worms are returned to 20°, we could observe the GFP first appearing in the pseudocoelom, then getting successively less bright in the pseudocoelom and more obvious in vesicles in the coelomocytes, before finally disappearing altogether (Figure 2). This suggests that the GFP is taken up and gets degraded, or is rendered otherwise nonfluorescent, by the coelomocytes.

Toxin-mediated ablation of coelomocytes: Coelomocytes are difficult to kill by laser ablation: apparently coelomocytes reported (via a personal communication in White 1988) to have been eliminated by laser ablation had actually recovered and retained some function (J. Kimble, personal communication). To assess the importance of coelomocyte function, we used a coelomocyte-specific promoter (P. Sengupta, personal communication; P. Loria and O. Hobert, personal communication) to express a variant diphtheria toxin, DT-A_{K51E} (DeLange *et al.* 1979). We verified the absence of the coelomocytes by examining the anatomy of *dpy-20; arIs37[*p*myo-3::ssGFP]; arEx218[pcc1::DT-*A_{K51E}*]* hermaphrodites and the fate of the secreted GFP (materials and methods). Most hermaphrodites lacked all six coelomocytes and accumulated GFP in the pseudocoelom (Figure 1G), confirming that GFP in the pseudocoelom is removed primarily by coelomocytes. We did not observe any effect on the viability or motility of this strain and were easily able to maintain the extragenic array for several generations, suggesting there is not a strong selection against it. We conclude that coelomocyte function, and in particular endocytosis by coelomocytes, is not necessary for viability and fertility of worms under normal laboratory conditions.

Involvement of genes known to function in membrane trafficking in endocytosis by coelomocytes: We tested whether proteins that are thought to function in membrane trafficking in other systems, directly or indirectly, play a major role in endocytosis by coelomocytes. We reduced or eliminated the activity of these genes in the *arIs37[*p*myo-3::ssGFP]* worms, either by using characterized mutant alleles or through the use of RNA-mediated interference (materials and methods). We assayed the effect on coelomocytes by qualitatively examining the level of GFP in the pseudocoelom and the number and size of vesicles containing GFP in the coelomocytes.

Conventional mutations tested: Because in the *arIs37 [*p*myo-3::ssGFP]* hermaphrodites we could reliably score only older larvae and adults for endocytosis by coelomocytes, we used only mutant alleles that did not result in zygotic lethality. We tested the effect on coelomocyte endocytosis of several genes that are known to affect membrane trafficking (*snt-1*, *unc-26*, *unc-11*, *unc-13*, *unc-64*, *unc-101*, *dyn-1*, *pod-1*, *unc-104*, *ced-2*, *ced-5*, *nrf-5*, *nrf-6*) and others that might influence the actin cytoskeleton (*unc-60*, *unc-115*, *cyk-1*, *mig-2*, *unc-73*; Table 1), as well as various miscellaneous mutations used for strain constructions (Table 1 legend). None of the mutations

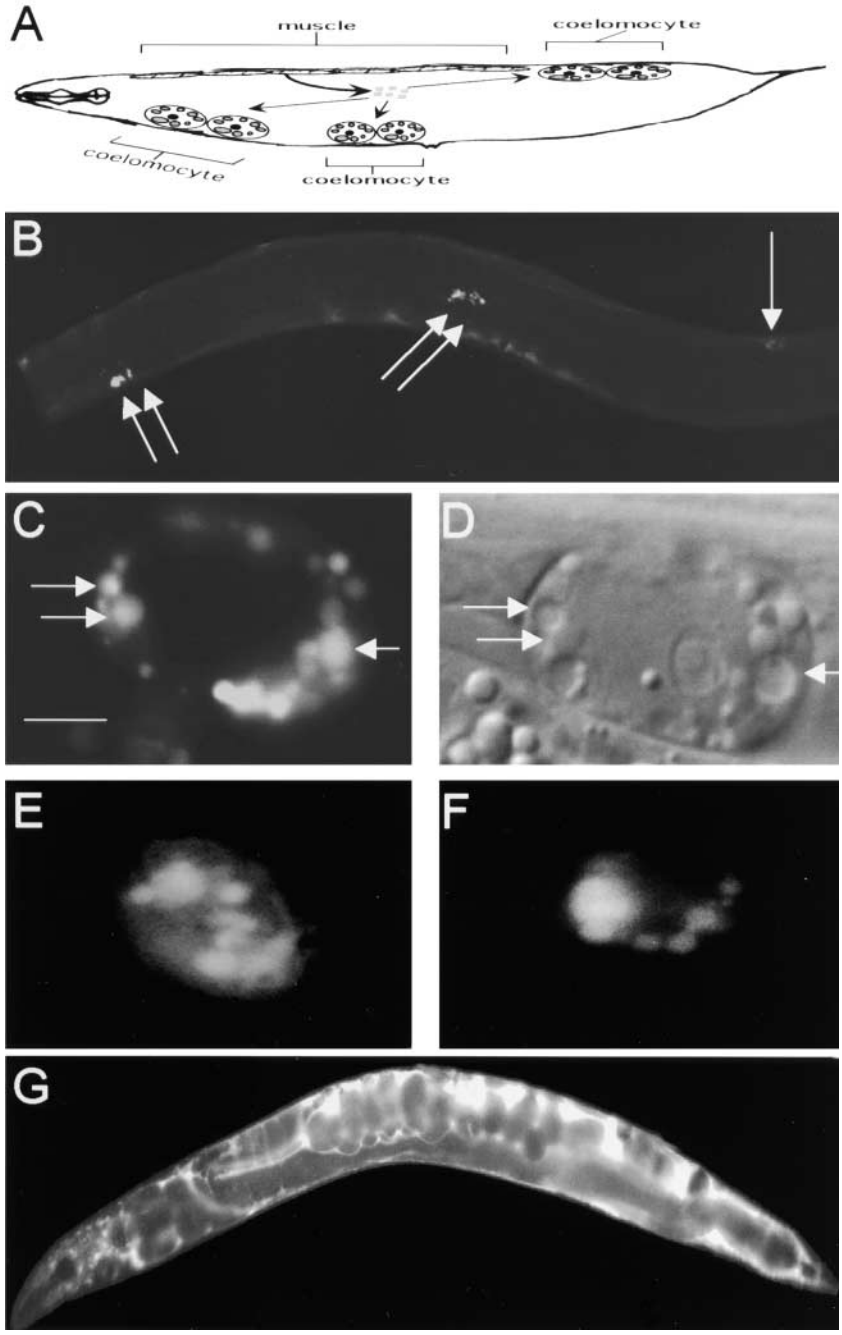

Figure 1.—Coelomocyte uptake of substances introduced into the pseudocoelom. Schematic drawing (A), epifluorescence (B and C), and Nomarski (D) micrographs of a *dpy-20(e1282); arIs37[*p*myo-3::ssGFP]* hermaphrodite. (E and F) Epifluorescence micrographs of a coelomocyte from an N2 hermaphrodite injected with FITC-conjugated BSA and rhodamine-conjugated dextran (M_r 40,000), respectively. (G) Epifluorescence micrograph of a *dpy-20(e1282); arIs37[*p*myo-3::ssGFP]; arEx218 [pcc1::DT-*A_{K51E}*]* hermaphrodite in which the coelomocytes have been ablated by expression of Diphtheria toxin. B and G are low magnification images of whole worms (anterior is to the left). Note the presence of some GFP in the pseudocoelom and in the coelomocytes (five are seen) in B and the accumulation of GFP in the pseudocoelom in G. (C and D) Higher magnification fluorescence and Nomarski images of the same coelomocyte, respectively. Arrows indicate the coelomocytes in B and vesicles filled with GFP in C and D. The shading represents GFP in A. B, C, and D have already been published (Fares and Greenwald 2001). Bar, 3.7 μm in C.

tested, except for *dyn-1(ky51ts)* (see below), resulted in a noticeable Cup phenotype. Where null alleles were used, we can conclude that the activity of the gene tested is not required for coelomocyte endocytosis. Where hypomorphic alleles were used, it remains possible that the lack of a Cup phenotype reflects residual gene activity.

dyn-1(ky51ts) is a temperature-sensitive mutation in dynamin, a large GTPase that regulates an early step in endocytosis and is involved in other cellular processes (Clark *et al.* 1997). At the permissive temperature, 20°, *dpy-20(e1282); dyn-1(ky51ts); arIs37[*p*myo-3::ssGFP]* worms appear indistinguishable from *dpy-20(e1282); arIs37 [*p*myo-3::ssGFP]* worms. However, *dpy-20(e1282); dyn-1 (ky51ts); arIs37[*p*myo-3::ssGFP]* worms that were shifted to 25° soon start displaying a Cup phenotype, characterized by accumulation of GFP in their pseudocoelom and a greatly reduced number of vesicles in coelomocytes (Figure 3).

RNAi: We tested several genes (Table 2) that encode proteins that are homologous, or have domains homologous, to proteins known to function in membrane trafficking. For *rme-1* and *cup-5*, RNAi was very effective and caused a phenotype that is essentially identical to that seen for null mutations in those genes (see below). *vps-34*, *sec-5*, and *sec-8* also showed a very strong accumulation of GFP in the pseudocoelom of F_1 worms, while

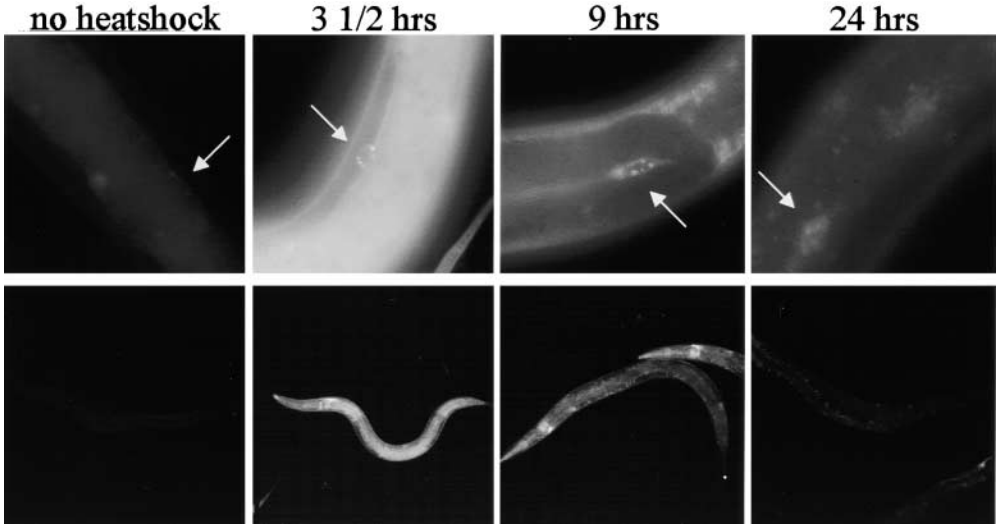

FIGURE 2.—Behavior of ssGFP after its expression and secretion by heat shock in *dpy-20(e1282); arIs36[*p*hsp::ssGFP]* hermaphrodites. Worms were grown at 20° (no heat shock), heat-shocked at 33° for 30 min, and put back at 20° for the indicated times shown above the micrographs. The top row of micrographs is at a higher magnification than those in the bottom row. Arrows indicate coelomocytes.

the accumulation of GFP in worms injected with *vps-54* and *clh-15* double-stranded RNA (dsRNA) was much weaker, but noticeably higher than in mock-injected worms.

When Cup RNAi phenotypes were observed, it was only in the F_1 progeny of parents that had been injected with double-stranded RNA. The injection method appeared to work best for several genes tested: when we

TABLE 1

Alleles tested for effects on coelomocyte endocytosis

Genes (alleles)[a]	Type of allele	Protein encoded	Reference
snt-1(n2665)	Null	Synaptotagmin	NONET *et al.* (1993)
unc-26(e205)	Null	Synaptojanin	HARRIS *et al.* (2000)
unc-11(e47)	Null	AP180	NONET *et al.* (1999)
unc-13(e51)[b]	Hypomorph	C1/C2 domains	RICHMOND *et al.* (1999)
unc-64(e246)	Hypomorph	Syntaxin	SAIFEE *et al.* (1998)
unc-101(m1)	Null	μ1 (AP1)	LEE *et al.* (1994)
dyn-1(ky51ts)	Hypomorph	Dynamin	CLARK *et al.* (1997)
pod-1(ye11)[c]	Null	Coronin	RAPPLEYE *et al.* (1999)
unc-104(e1265)	Hypomorph	Kinesin HC	OTSUKA *et al.* (1991)
ced-2(e1752)	Hypomorph	CrkII	REDDIEN and HORVITZ (2000)
ced-5(n1812)	Null	DOCK180	WU and HORVITZ (1998)
nrf-5(sa513)	Unknown	Novel	CHOY and THOMAS (1999)
nrf-6(sa525)	Null	Novel	CHOY and THOMAS (1999)
unc-60(e677)[d]	Hypomorph	Actin binding	MCKIM *et al.* (1994)
unc-115(e2225)	Hypomorph	Actin binding	LUNDQUIST *et al.* (1998)
cyk-1(or36)[e]	Hypomorph	Formin	SWAN *et al.* (1998)
mig-2(mn28)	Null	Rho	ZIPKIN *et al.* (1997)
unc-73(e936)	Hypomorph	Trio/kalirin	STEVEN *et al.* (1998)

All worms were checked at 20°, except for temperature-sensitive mutants that were checked at 25°. Many worms also had *dpy-20(e1282)*.

[a] Other mutations tested include *bli-5(e518)*, *ced-9(n1950)*, *dpy-5(e61)*, *dpy-7(e88)*, *dpy-9(e12)*, *dpy-10(e128)*, *dpy-11(e224)*, *dpy-13(e184)*, *dpy-14(e188)*, *dpy-17(e164)*, *dpy-18(e364)*, *dpy-24(s71)*, *eat-1(e2343)*, *eat-20(nc4)*, *emb-29(g52)*, *emb-29(b262)*, *glp-4(bn2ts)*, *him-5(e1490)*, *lag-2(q420ts)*, *lin-1(n304)*, *lin-1(e1275)*, *lin-10(e1439)*, *mab-18(bx23)*, *rol-6(e187)*, *sma-1(e30)*, *sma-3(e491)*, *spg-(e2335)*, *sqt-3(sc63)*, *unc-4(e120)*, *unc-6(e78)*, *unc-6(n102)*, *unc-17(e245)*, *unc-18(e81)*, *unc-25(e156)*, *unc-29(e1072)*, *unc-30(e191)*, *unc-31(e169)*, *unc-32(e189)*, *unc-33(e204)*, *unc-34(e566)*, *unc-36(e251)*, *unc-39(e257)*, *unc-42(e270)*, *unc-54(e190)*, *unc-69(e587)*, *unc-76(e911)*, *unc-78(e1217)*, *unc-97(su110)*.

[b] *unc-13(e1091)* was also checked.

[c] *unc-32(e189) pod-1(ye11); arIs37[*p*myo-3::ssGFP]* worms were isolated and checked from *unc-32(e189) pod-1(ye11)/qC1; arIs37[*p*myo-3::ssGFP]* parents.

[d] *unc-60(e723)* and *unc-60(m35)* were also checked.

[e] *cyk-1(or36) unc-36(e251); arIs37[*p*myo-3::ssGFP]* worms were isolated and checked from *cyk-1(or36) unc-36(e251)/qC1; arIs37[*p*myo-3::ssGFP]* parents.

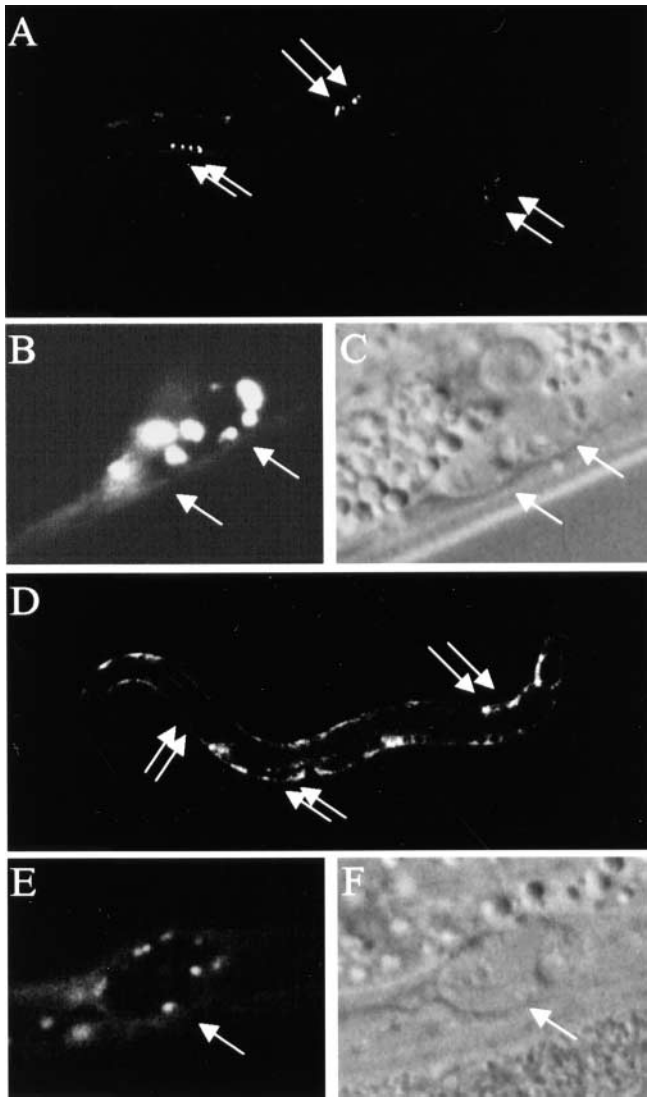

FIGURE 3.—Effect of *dyn-1(ky51ts)* on coelomocyte endocytosis. All images are of *dpy-20(e1282); dyn-1(ky51ts); arIs37[*p*myo-3::ssGFP]* hermaphrodites grown at 20° (A–C) or shifted for 8 hr to 25° (D–F). (B and C; E and F) Higher magnification fluorescence and Nomarski images of the same coelomocytes, respectively. Arrows indicate coelomocytes (not visible in D due to the decreased uptake of GFP). Note the presence of fewer and smaller vesicles in the coelomocytes shown in E as compared to those shown in B.

tried soaking worms in double-stranded RNA (TABARA *et al.* 1998), we saw little or no effect (data not shown). Feeding worms bacteria expressing double-stranded RNA (TIMMONS and FIRE 1998) had a similar effect to RNA injection, but was less efficient (data not shown). We therefore could not use RNAi to assay several genes (*e.g.*, clathrin heavy chain, RAB-5, and RAB-11) that are known to be involved in endocytosis but that resulted in lethality in the F_1 progeny of the injected worms and/or in sterility in the injected worms.

Screen for new mutants defective in endocytosis by coelomocytes: We mutagenized *dpy-20(e1282); arIs37 [*p*myo-3::ssGFP]* worms with EMS and identified 55 viable mutants that displayed differences in endocytosis by coelomocytes compared to the parent strain. Of these mutations, 53 are recessive and define 14 complementation groups (Table 3; MATERIALS AND METHODS). We found that 3 of these complementation groups correspond to *rme-1 rme-6* and *rme-8*, genes defined in a screen for *r*eceptor-*m*ediated *e*ndocytosis of yolk (GRANT and HIRSH 1999). The two dominant mutations identified proved to be dominant-negative alleles of *rme-1* (GRANT *et al.* 2001). On the basis of mapping data, *inter se* complementation tests, and complementation tests with other selected genes in the same region (see MATERIALS AND METHODS), the remainder of the 11 complementation groups appear to define new genes, which we have named *cup*.

The coelomocyte phenotype of *cup* mutants: In all the mutants isolated, except *cup-5(ar465)*, the gross phenotype we observed was the accumulation of GFP in the pseudocoelom, suggesting a decrease in, or the absence of, endocytosis in coelomocytes. *cup-5(ar465)* worms had the opposite phenotype: reduced GFP in the pseudocoelom and greatly intensified GFP accumulation in coelomocytes, suggesting enhanced uptake and decreased degradation of GFP by coelomocytes (FARES and GREENWALD 2001).

We examined more closely the phenotype of the coelomocytes in mutant worms grown at 20° (Figure 4). Interestingly, the coelomocytes exhibit a whole range of phenotypes, suggesting that the endocytic pathway is perturbed at several steps and/or in several ways. We show some examples in Figure 4, including almost no uptake of GFP by coelomocytes in *cup-10(ar479)* worms (Figure 4B), the accumulation of small peripheral GFP-filled compartments in *cup-1(ar478)* worms (Figure 4C), the accumulation of several vesicles that are full of GFP (indistinguishable from the wild-type profile at this level of analysis) in *cup-11(ar472)* worms (Figure 4D), the appearance of large vacuoles with little GFP in *cup-8(ar466)* worms (Figure 4E), and the accumulation of GFP in large vacuoles in *cup-5(ar465)* worms (Figure 4F).

Additional phenotypes: We checked all of the mutants for phenotypes that might indicate defects in endocytosis by other cell types (Table 3). On the basis of our limited analysis, seven of the complementation groups were deficient only in endocytosis by coelomocytes, and seven also affected endocytosis by other tissues.

Uncoordinated phenotype: An Unc phenotype might be indicative of defects in synaptic vesicle recycling (for example, NONET *et al.* 1993, 1999; HARRIS *et al.* 2000). The only *cup* mutants that display an Unc defect are the two alleles of *cup-7*, which move very slowly and have a slight tendency to curl. All of the other mutants have normal movement.

Oocyte uptake of yolk: Accumulation of yolk in the pseudocoelom may be visualized as bright birefringence using Nomarski microscopy (KIMBLE and SHARROCK

TABLE 2

RNA interference test of coelomocyte endocytosis

Clone	ORF	Protein	Other phenotypes	Reference
		A. Cup phenotype seen		
yk271a1	W06H8.1	RME-1 (EH domain)	Gut vacuoles	Grant *et al.* (2001)
yk561c9	R13A5.1	CUP-5 (mucolipin-1)	—	Fares and Greenwald (2001)
yk2e6	B0025.1	VPS-34 (PI-3 kinase)	Slow growth	Stack and Emr (1994)
yk557a2	C07H4.2	CLH-15 (chloride channel)	—	Wang *et al.* (2000)
yk3e11	T21C9.2	VPS-54	—	Conboy and Cyert (2000)
yk38b5	Y106G6H.7	SEC-8 (exocyst)	Gut vacuoles, slow growth	TerBush *et al.* (1996)
yk52b9	T23G7.4	SEC-5 (exocyst)	Gut vacuoles	TerBush *et al.* (1996)
		B. Cup phenotype not seen		
yk66d7	H22K11.1	ASP-3 (aspartic protease)	—	Tcherepanova *et al.* (2000)
yk98g7	C03B1.12	LMP-1 (LAMP)	—	Kostich *et al.* (2000)
yk397e6	F58G6.1	Amphiphysin	—	Lichte *et al.* (1992)
yk326a2	F45E1.17	Syndapin	—	Qualmann *et al.* (1999)
yk261h11	Y55D9A.1	SEC-7, PH[a] domain	—	Achstetter *et al.* (1988)
yk392e11	K06H7.4	GRP-1/ SEC-7, PH[a] domain	—	Achstetter *et al.* (1988)
yk33e1	M02B7.5	SEC-7 domain	—	Achstetter *et al.* (1988)
yk61c3	T13F2.8	CAV-1 (caveolin)	—	Tang *et al.* (1997)
yk411g3	F36F2.4	Syntaxin 12/7	—	Jantsch-Plunger and Glotzer (1999)
PCR[b]	C01A2.1	Synaptobrevin-like	—	Baumert *et al.* (1989)
PCR[b]	F23H12.1	Synaptobrevin	—	Baumert *et al.* (1989)
yk481g10	T04C10.2	Epsin	—	Chen *et al.* (1998)
yk21f1	C04F6.4	DAip1 (WD40 repeats)	Uncoordinated movement	Konzok *et al.* (1999)
yk228a8	W03C9.3	RAB-7	—	Chavrier *et al.* (1990)
yk74d9	W09G10.4	ADAPTIN (AP3)	—	Simpson *et al.* (1997)
yk507b6	T05B11.3	Clathrin light chain	—	Creutz and Harrison (1984)
yk63d5	M01D7.2	SCAMP	—	Singleton *et al.* (1997)
yk445h11	C01F6.1	Copine	—	Creutz *et al.* (1998)
yk71c12	T07A9.10	SEC-1	—	Aalto *et al.* (1991)
yk99b4	R11B5.1	Drainin	—	Becker *et al.* (1999)
yk5h12	ZK370.3	Hip1R	—	Seki *et al.* (1998)
yk304g6	R01H10.3[c]	Coronin	—	Maniak *et al.* (1995)
yk81h9	F25H2.5	Nm23	Sterile F_1	Steeg *et al.* (1988)
PCR[b]	F55A3.6	Nm23	—	Steeg *et al.* (1988)

dsRNA was injected into *dpy-20(e1282); arIs37[*p*myo-3::ssGFP]* worms and the resulting F_1 were checked at 20°. ORF, open reading frame.

[a] PH, pleckstrin homology.

[b] PCR signifies that because no cDNA clone was available for this ORF, we amplified a portion of that ORF using two primers complementary to its ends and with sequences for T3 and T7 polymerase added to the primers' ends, respectively. Double-stranded RNA was made directly from this amplified fragment.

[c] R01H10.3 is distinct from POD-1, the second coronin in *C. elegans.* dsRNA from yk304g6 was also injected into the *unc-32(e189) pod-1(ye11)/qC1; arIs37[*p*myo-3::ssGFP]* worms and the homozygous *pod-1(ye11)* F_1 checked, similarly with no effect on endocytosis by coelomocytes.

1983). Using this assay, hermaphrodites bearing *cup-1(ar478)*, *cup-3(ar496)*, *cup-6(ar513)*, or *cup-7(ar492)* accumulated more yolk granules in the pseudocoelom than the wild-type parent strains.

Intestinal uptake: Rhodamine-dextran (M_r 40,000) present in the growth medium is endocytosed by intestinal cells. We examined the *cup* mutants for intestinal accumulation of rhodamine-dextran in the presence or absence of cholesterol, a membrane component that must be added to the growth medium for continued growth of *C. elegans* in culture (Brenner 1974) and that is required for some endocytic pathways (Hoekstra and van IJzendoorn 2000). In the presence of supplemented cholesterol, only *rme-8(ar486)* was defective for uptake of rhodamine-dextran by intestinal cells. However, in the absence of supplemented cholesterol, both *cup-1(ar478)* and *rme-8(ar486)* showed a severe defect in rhodamine-dextran uptake in intestinal cells. The defect

TABLE 3

Coelomocyte uptake mutants

Gene	No. of alleles	Map position (interval)[a]	Other endocytic phenotypes[b]
cup-1	2	I (*unc-101* to *glp-4*)	Yolk, Int
cup-2	1	I (close to *dpy-24*)	—
rme-8	1	I (*unc-13* to *lin-10*)[c]	Yolk, Int
cup-3	5	II (*dpy-10* to *unc-4*)	Yolk
cup-4	1	III (*sma-3* to *unc-36*)	—
cup-5	1	III (*sma-3* to *unc-36*)	—
cup-6	2	III (ND)	Yolk
cup-7	2	IV (*lin-1* to *unc-33*)	Unc, Yolk
cup-8	3	V (*unc-34* to *unc-60*)	—
cup-9	15	V (*sma-1* to *unc-39*)	—
cup-10	1	V (*lag-2* to *let-478*)	—
rme-1	5	V (*unc-46* to *dpy-11*)[d]	Yolk
cup-11	9	X (*mup-2* to *unc-6*)	—
rme-6	7	X (close to *unc-1*)[e]	Yolk

ND, not determined.

[a] See MATERIALS AND METHODS for mapping information.

[b] Other phenotypes checked were uncoordinated movement (Unc), yolk accumulation in the pseudocoelom (Yolk), and endocytosis by intestinal cells (Int). See RESULTS for details.

[c] ZHANG *et al.* (2001).

[d] GRANT *et al.* (2001).

[e] B. GRANT and D. HIRSH (personal communication).

appeared to fall in an anterior-posterior gradient, with cells in the posterior half showing almost no uptake of the rhodamine-dextran. This gradient might reflect the concentration of the ingested substance, which may progressively decrease during its passage through the lumen. Thus, in nonmutant worms, endocytosis is efficient enough so that posterior cells may still scavenge detectable rhodamine-dextran from the lumen, whereas in *cup-1* and *rme-8* mutants, endocytosis is sufficiently impaired that rhodamine-dextran accumulation cannot be seen.

DISCUSSION

We have shown that the coelomocytes continuously and efficiently endocytose fluid from the pseudocoelom and are not essential for the survival of the animal. We used the ability of coelomocytes to endocytose the fluid-phase marker GFP from the pseudocoelom as the basis for identifying mutants defective in endocytosis. A reverse genetic approach, using RNA-mediated interference, established that certain known genes are required for coelomocyte endocytosis and that blocking endocytosis leads to a Cup phenotype. A forward genetic screen for mutants identified 14 *cup* genes, 11 of which appear to be new. Here, we discuss what we have learned about the process of endocytosis in coelomocytes from our genetic analysis and evaluate the potential of the *cup* mutant screen for identifying new endocytosis genes.

We found that many soluble compounds injected into the pseudocoelom are taken up by the coelomocytes. The compounds that did not get endocytosed can be divided into two categories. One category comprises compounds that appeared to associate with yolk granules, which appear to be excluded from coelomocytes (D. HALL, personal communication) due to their size, hydrophobicity, or some other, unknown, property. The other category has as yet a single member, FITC-dextran (M_r 2,000,000), which did not appear to associate with yolk granules; because a smaller dextran polymer was very efficiently endocytosed by coelomocytes, size may be an important factor in determining the ability of a compound to be taken up. One reason that size may be important is that there is an electron-dense glycocalyx

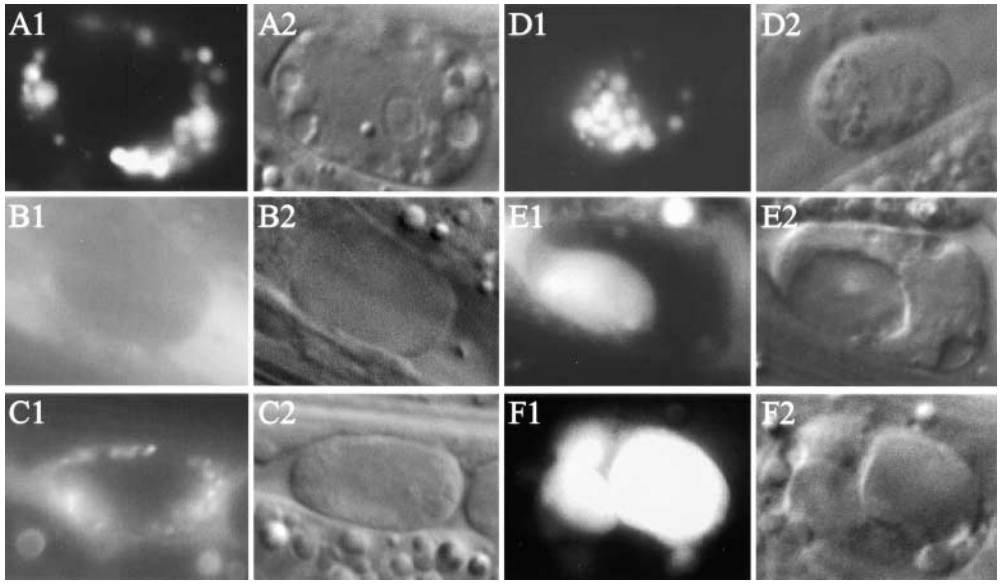

FIGURE 4.—Phenotype of coelomocytes in the various *cup* mutant hermaphrodites. Shown are the fluorescence (1) and corresponding Nomarski micrographs (2) of wild-type worms (A) and worms carrying the following mutations: (B) *cup-10(ar479)*, (C) *cup-1(ar478)*, (D) *cup-11(ar472)*, (E) *cup-8 (ar466)*, and (F) *cup-5(ar465)*. All worms also were *dpy-20 (e1282); arIs37[*p*myo-3::ssGFP]*. F has already been published (FARES and GREENWALD 2001).

or basement membrane surrounding each coelomocyte (White 1988; D. Hall, personal communication), which may in effect act as a sieve. Analysis of uptake at the electron microscopic level may help resolve this issue.

The large number of compounds that were efficiently endocytosed raises the question of whether coelomocytes take up material from the pseudocoelom by constitutive pinocytosis and/or by scavenger receptors displaying a broad spectrum of ligand recognition (Pearson 1996). The results of our genetic analysis in *C. elegans* so far favor the possibility of a receptor-mediated mechanism.

First, the reduction or elimination of dynamin function led to an endocytosis defect in coelomocytes. Dynamin is known to function in the maturation and/or scission of the clathrin pit (Sever *et al.* 2000; Hill *et al.* 2001) and in endocytosis through caveolae (Henley *et al.* 1998). Clathrin itself is very strongly expressed in coelomocytes (Y. Zhang and D. Hirsh, personal communication) and numerous coated pits and vesicles are found on the surface of these cells (White 1988). This suggests that clathrin-mediated endocytosis may be the major pathway in coelomocytes. An alternative explanation is that in the coelomocytes of *C. elegans*, dynamin might also be used in other pathways of endocytosis that do not involve receptors.

Second, *rme-1* was identified in our genetic screen for *cup* mutants. RME-1 has been shown to be involved in membrane (and membrane protein) recycling to the plasma membrane (Grant *et al.* 2001; Lin *et al.* 2001). In *rme-1* null mutants, the Cup defect is more visible in older worms, as might be the case if scavenger receptors must be depleted from the plasma membrane before a Cup defect is seen. Alternatively, the Cup defect of *rme-1* mutant worms could be due to a general depletion of bulk membrane from the surface or due to some function of RME-1 in these cells other than recycling.

Some genes encoding other proteins with characterized roles in vesicle trafficking were also identified as playing roles in coelomocyte endocytosis by virtue of a Cup phenotype in RNAi experiments. *vps-34* encodes phosphoinositide 3-kinase (PI-3 kinase), a protein that regulates multiple steps in endocytosis (Backer 2000). *sec-5* and *sec-8* encode homologs of the yeast Sec5p and Sec8p, members of the exocyst complex. *S. cerevisiae sec* mutants, including *sec5* and *sec8*, which accumulate proteins in secretory vesicles, are all defective in endocytosis (Riezman 1985). Vps54p in *S. cerevisaie* is involved in vacuolar trafficking (Conboy and Cyert 2000). *clh-15* encodes a chloride channel that in human cells is involved in receptor-mediated endocytosis (Wang *et al.* 2000); the reduction in endocytosis in *clh-15(RNAi)* worms is less severe than for other genes that affect endocytosis by coelomocytes, possibly because of the existence of multiple genes that encode chloride channels in *C. elegans* (Nehrke *et al.* 2000).

Many genes, some of which are known to function in membrane trafficking, did not seem to be involved in endocytosis by coelomocytes. For example, null alleles of *snt-1* Synaptotagmin, *unc-26* Synaptojanin, *unc-11* AP180, and *unc-101* AP1 perturb membrane trafficking in neurons and other tissues in *C. elegans* but do not cause a Cup phenotype. While it is possible that some of the genes tested may not be expressed in coelomocytes, it is also possible that they are expressed in coelomocytes but only affect one pathway used by coelomocytes to internalize fluid. Furthermore, several of the genes tested have relatives in the *C. elegans* genome that may afford functional redundancy.

We screened for and identified mutations involved in the uptake of GFP by coelomocytes and identified alleles of 11 new *cup* genes and 3 previously identified *rme* genes. In this initial screen, we selected for homozygous viable and fertile Cup mutants. It is likely, therefore, that we have not identified genes that function in endocytosis and that regulate essential processes, like cell-cell signaling during embryonic development. Indeed, during the course of this screen, we saw some indication that there may be a category of endocytosis mutants that are also associated with zygotic or maternal-effect lethality. For several of the *cup* genes, we identified only single alleles, so we have not achieved saturation for this screen. Some of the alleles we recovered may prove to be non-null alleles of essential genes.

The *cup* screen described here and the *rme* screen described by B. Grant and D. Hirsh (1999) are both powerful screens for endocytosis mutants and thus far have yielded largely complementary sets of genes. We have tested the available *cup* genes for yolk accumulation, and B. Grant and D. Hirsh (personal communication) have tested most of the *rme* genes for a Cup phenotype. Although neither screen has been conducted to saturation, the data so far suggest that roughly one-third to one-half of the genes affect both yolk uptake by oocytes and pseudocoelomic GFP uptake by coelomocytes.

Both the Rme and the Cup screens have identified genes that play important roles in endocytosis in animal cells that do not appear to have homologs in yeast. As mentioned above, *rme-1*, which was identified in both the Rme and Cup screens, appears to be involved in membrane (and membrane protein) recycling to the plasma membrane (Grant *et al.* 2001; Lin *et al.* 2001). *rme-8*, also identified in both the Rme and Cup screens, appears to be involved in endocytic vesicle trafficking (Zhang *et al.* 2001). Finally, *cup-5*, which was identified solely by the Cup screen, encodes the *C. elegans* homolog of human mucolipin-1 (Fares and Greenwald 2001). Loss of human mucolipin-1 underlies Mucolipidosis Type IV, a lysosomal storage disease that results in severe developmental neuropathology (Bargal *et al.* 2000; Bassi *et al.* 2000; Sun *et al.* 2000). As we report elsewhere (Fares and Greenwald 2001), our analysis has revealed that there are striking parallels between the cellular

phenotypes and endocytosis defects of *cup-5* mutant *C. elegans* and cells from patients with Mucolipidosis Type IV. We expect that at least some other *cup* genes will also prove to be components of the endocytosis machinery that are unique to animal cells.

Finally, what is the function of the coelomocytes of *C. elegans*? In many invertebrates, coelomocytes/hemocytes mediate the cellular immunity of the organism (Pancer *et al.* 1999). We have not found evidence that the coelomocytes of *C. elegans* provide a potent defense against bacterial infection; as few as six bacterial cells (OP50) injected into the pseudocoelom can multiply and kill the worm (H. Fares and I. Greenwald, unpublished observations). This function for coelomocytes may be better explored by comparing the susceptibility of wild type *vs.* worms lacking coelomocytes to infection; to date, however, the only microorganism reported to invade the pseudocoelom of worms is the fungus *Drechmeria coniospora*, which extends its hyphae into the pseudocoelom (Jansson 1994). However, it may be that in *C. elegans*, the coelomocyte functions more like a liver. The pseudocoelomic fluid serves as the circulatory system for nutrients that are taken up, ingested, degraded, and secreted into the pseudocoelom by the intestinal cells. It is possible that the coelomocytes reprocess that fluid to detoxify it of harmful ingested substances. In that event, it is likely that the absence of coelomocytes would not be harmful to worms grown under laboratory conditions. It is now possible to test this by comparing the susceptibility of wild type *vs.* worms lacking coelomocytes to toxic material introduced into the growth medium or secreted by bacterial pathogens (Tan and Ausubel 2000). With the availability of worms that lack coelomocytes and worms that are defective in endocytosis by coelomocytes, we are now in a better position to determine the biological function of these cells in *C. elegans*.

We are grateful to David Hirsh for inspiring our interest in coelomocytes, Barth Grant and Yinhua Zhang for helpful reagents and discussions throughout the project, Piali Sengupta for the coelomocyte-specific promoter and Paula Loria and Oliver Hobert for additional information about it, David Hall for communicating unpublished observations, and John Collier for the Diphtheria toxin clones. We also thank Alan Coulson and Yuji Kohara for providing cosmids, strains, and cDNA clones, Richard Ruiz and Ilya Temkin for excellent technical assistance, Barth Grant, Oliver Hobert, and Sophie Jarriault for critical reading of the manuscript, and past and present members of the Greenwald, Hirsh, and Hobert laboratories for helpful discussions. Some strains were provided by the Caenorhabditis Genetics Center, which is funded by the National Institutes of Health National Center for Research Resources (NCRR). I.G. is an Investigator of the Howard Hughes Medical Institute. H.F. was a Postdoctoral Associate of the HHMI and was also supported by an award from the Metropolitan Life Foundation to I.G.

LITERATURE CITED

Aalto, M. K., L. Ruohonen, K. Hosono and S. Keranen, 1991 Cloning and sequencing of the yeast *Saccharomyces cerevisiae SEC1* gene localized on chromosome IV. Yeast **7:** 643–650.

Achstetter, T., A. Franzusoff, C. Field and R. Schekman, 1988 *SEC7* encodes an unusual, high molecular weight protein required for membrane traffic from the yeast Golgi apparatus. J. Biol. Chem. **263:** 11711–11717.

Backer, J. M., 2000 Phosphoinositide 3-kinases and the regulation of vesicular trafficking. Mol. Cell. Biol. Res. Commun. **3:** 193–204.

Bacon, R. A., C. J. Cohen, D. A. Lewin and I. Mellman, 1994 *Dictyostelium discoideum* mutants with temperature-sensitive defects in endocytosis. J. Cell Biol. **127:** 387–399.

Bargal, R., N. Avidan, E. Ben-Asher, Z. Olender, M. Zeigler *et al.*, 2000 Identification of the gene causing Mucolipidosis Type IV. Nat. Genet. **26:** 118–123.

Bassi, M. T., M. Manzoni, E. Monti, M. T. Pizzo, A. Ballabio *et al.*, 2000 Cloning of the gene encoding a novel integral membrane protein, mucolipidin—and identification of the two major founder mutations causing Mucolipidosis Type IV. Am. J. Hum. Genet. **67:** 1110–1120.

Baumert, M., P. R. Maycox, F. Navone, P. De Camilli and R. Jahn, 1989 Synaptobrevin: an integral membrane protein of 18,000 daltons present in small synaptic vesicles of rat brain. EMBO J. **8:** 379–384.

Becker, M., M. Matzner and G. Gerisch, 1999 Drainin required for membrane fusion of the contractile vacuole in Dictyostelium is the prototype of a protein family also represented in man. EMBO J. **18:** 3305–3316.

Bossinger, O., and E. Schierenberg, 1996 The use of fluorescent marker dyes for studying intercellular communication in nematode embryos. Int. J. Dev. Biol. **40:** 431–439.

Brenner, S., 1974 The genetics of *Caenorhabditis elegans*. Genetics **77:** 71–94.

Chalfie, M., Y. Tu, G. Euskirchen, W. W. Ward and D. C. Prasher, 1994 Green fluorescent protein as a marker for gene expression. Science **263:** 802–805.

Chavrier, P., R. G. Parton, H. P. Hauri, K. Simons and M. Zerial, 1990 Localization of low molecular weight GTP binding proteins to exocytic and endocytic compartments. Cell **62:** 317–329.

Chen, H., S. Fre, V. I. Slepnev, M. R. Capua, K. Takei *et al.*, 1998 Epsin is an EH-domain-binding protein implicated in clathrin-mediated endocytosis. Nature **394:** 793–797.

Chitwood, B. G., and M. B. Chitwood, 1974 *Introduction to Nematology*. University Park Press, Baltimore.

Choy, R. K., and J. H. Thomas, 1999 Fluoxetine-resistant mutants in *C. elegans* define a novel family of transmembrane proteins. Mol. Cell **4:** 143–152.

Chvatchko, Y., I. Howald and H. Riezman, 1986 Two yeast mutants defective in endocytosis are defective in pheromone response. Cell **46:** 355–364.

Clark, S. G., D. L. Shurland, E. M. Meyerowitz, C. I. Bargmann and A. M. van der Bliek, 1997 A dynamin GTPase mutation causes a rapid and reversible temperature-inducible locomotion defect in *C. elegans*. Proc. Natl. Acad. Sci. USA **94:** 10438–10443.

Colbaugh, P. A., C. Y. Kao, S. P. Shia, M. Stookey and R. K. Draper, 1988 Three new complementation groups of temperature-sensitive Chinese hamster ovary cell mutants defective in the endocytic pathway. Somat. Cell Mol. Genet. **14:** 499–507.

Conboy, M. J., and M. S. Cyert, 2000 Luv1p/Rki1p/Tcs3p/Vps54p, a yeast protein that localizes to the late Golgi and early endosome, is required for normal vacuolar morphology. Mol. Biol. Cell **11:** 2429–2443.

Creutz, C. E., and J. R. Harrison, 1984 Clathrin light chains and secretory vesicle binding proteins are distinct. Nature **308:** 208–210.

Creutz, C. E., J. L. Tomsig, S. L. Snyder, M. C. Gautier, F. Skouri *et al.*, 1998 The copines, a novel class of C2 domain-containing, calcium-dependent, phospholipid-binding proteins conserved from Paramecium to humans. J. Biol. Chem. **273:** 1393–1402.

DeLange, R. J., L. C. Williams, R. E. Drazin and R. J. Collier, 1979 The amino acid sequence of fragment A, an enzymically active fragment of diphtheria toxin. III. The chymotryptic peptides, the peptides derived by cleavage at tryptophan residues, and the complete sequence of the protein. J. Biol. Chem. **254:** 5838–5842.

Fares, H., and I. Greenwald, 2001 Regulation of endocytosis by CUP-5, the *Caenorhabditis elegans* mucolipin-1 homologue. Nat. Genet. **28:** 64–68.

Fire, A., 1986 Integrative transformation of *Caenorhabditis elegans*. EMBO J. **5:** 2673–2680.

Fire, A., S. Xu, M. K. Montgomery, S. A. Kostas, S. E. Driver *et al.*, 1998 Potent and specific genetic interference by double-stranded RNA in *Caenorhabditis elegans*. Nature **391:** 806–811.

Fitzgerald, K., and I. Greenwald, 1995 Interchangeability of *Caenorhabditis elegans* DSL proteins and intrinsic signalling activity of their extracellular domains *in vivo*. Development **121:** 4275–4282.

Grant, B., and I. Greenwald, 1997 Structure, function, and expression of SEL-1, a negative regulator of LIN-12 and GLP-1 in *C. elegans*. Development **124:** 637–644.

Grant, B., and D. Hirsh, 1999 Receptor-mediated endocytosis in the *Caenorhabditis elegans* oocyte. Mol. Biol. Cell **10:** 4311–4326.

Grant, B., Y. Zhang, M.-C. Paupard, S. X. Lin, D. H. Hall *et al.*, 2001 Evidence that RME-1, a conserved *C. elegans* EH domain protein, functions in endocytic recycling. Nat. Cell Biol. **3:** 573–579.

Han, M., and P. W. Sternberg, 1991 Analysis of dominant-negative mutations of the *Caenorhabditis elegans let-60* ras gene. Genes Dev. **5:** 2188–2198.

Harris, T. W., E. Hartwieg, H. R. Horvitz and E. M. Jorgensen, 2000 Mutations in synaptojanin disrupt synaptic vesicle recycling. J. Cell Biol. **150:** 589–600.

Henley, J. R., E. W. Krueger, B. J. Oswald and M. A. McNiven, 1998 Dynamin-mediated internalization of caveolae. J. Cell Biol. **141:** 85–99.

Hill, E., J. vand der Kaay, C. P. Downes and E. Smythe, 2001 The role of dynamin and its binding partners in coated pit invagination and scission. J. Cell Biol. **152:** 309–323.

Hobbie, L., A. S. Fisher, S. Lee, A. Flint and M. Krieger, 1994 Isolation of three classes of conditional lethal Chinese hamster ovary cell mutants with temperature-dependent defects in low density lipoprotein receptor stability and intracellular membrane transport. J. Biol. Chem. **269:** 20958–20970.

Hoekstra, D., and S. C. van IJzendoorn, 2000 Lipid trafficking and sorting: how cholesterol is filling gaps. Curr. Opin. Cell Biol. **12:** 496–502.

Hosono, R., K. Hirahara, S. Kuno and T. Kurihara, 1982 Mutants of *Caenorhabditis elegans* with dumpy and rounded head phenotype. J. Exp. Zool. **235:** 409–421.

Huang, K. M., K. D'Hondt, H. Riezman and S. K. Lemmon, 1999 Clathrin functions in the absence of heterotetrameric adaptors and AP180-related proteins in yeast. EMBO J. **18:** 3897–3908.

Jansson, H.-B., 1994 Adhesion of conidia of *Drechmeria coniospora* to *Caenorhabditis elegans* wild type and mutants. J. Nematol. **26:** 430–435.

Jantsch-Plunger, V., and M. Glotzer, 1999 Depletion of syntaxins in the early *Caenorhabditis elegans* embryo reveals a role for membrane fusion events in cytokinesis. Curr. Biol. **9:** 738–745.

Jones, D., R. H. Russnak, R. J. Kay and E. P. Candido, 1986 Structure, expression, and evolution of a heat shock gene locus in *Caenorhabditis elegans* that is flanked by repetitive elements. J. Biol. Chem. **261:** 12006–12015.

Kimble, J., and W. J. Sharrock, 1983 Tissue-specific synthesis of yolk proteins in *Caenorhabditis elegans*. Dev. Biol. **96:** 189–196.

Konzok, A., I. Weber, E. Simmeth, U. Hacker, M. Maniak *et al.*, 1999 DAip1, a Dictyostelium homologue of the yeast actin-interacting protein 1, is involved in endocytosis, cytokinesis, and motility. J. Cell Biol. **146:** 453–464.

Kostich, M., A. Fire and D. M. Fambrough, 2000 Identification and molecular-genetic characterization of a LAMP/CD68-like protein from *Caenorhabditis elegans*. J. Cell Sci. **113:** 2595–2606.

Krieger, M., 1986 Isolation of somatic cell mutants with defects in the endocytosis of low-density lipoprotein. Methods Enzymol. **129:** 227–237.

Lander, E. S., L. M. Linton, B. Birren, C. Nusbaum, M. C. Zody *et al.*, 2001 Initial sequencing and analysis of the human genome. Nature **409:** 860–921.

Lee, J., G. D. Jongeward and P. W. Sternberg, 1994 *unc-101*, a gene required for many aspects of *Caenorhabditis elegans* development and behavior, encodes a clathrin-associated protein. Genes Dev. **8:** 60–73.

Lemmon, S. K., and L. M. Traub, 2000 Sorting in the endosomal system in yeast and animal cells. Curr. Opin. Cell Biol. **12:** 457–466.

Lichte, B., R. W. Veh, H. E. Meyer and M. W. Kilimann, 1992 Amphiphysin, a novel protein associated with synaptic vesicles. EMBO J. **11:** 2521–2530.

Lin, S. X., B. Grant, D. Hirsh and F. R. Maxfield, 2001 Rme-1 regulates the distribution and function of the endocytic recycling compartment in mammalian cells. Nat. Cell Biol. **3:** 567–572.

Lundquist, E. A., R. K. Herman, J. E. Shaw and C. I. Bargmann, 1998 UNC-115, a conserved protein with predicted LIM and actin-binding domains, mediates axon guidance in *C. elegans*. Neuron **21:** 385–392.

Maniak, M., R. Rauchenberger, R. Albrecht, J. Murphy and G. Gerisch, 1995 Coronin involved in phagocytosis: dynamics of particle-induced relocalization visualized by a green fluorescent protein tag. Cell **83:** 915–924.

Matyash, V., C. Geier, A. Henske, B. Gregan, S. Mukherjee *et al.*, 2001 Distribution and transport of cholesterol in *Caenorhabditis elegans*. Mol. Biol. Cell **12:** 1725–1736.

McKim, K. S., C. Matheson, M. A. Marra, M. F. Wakarchuk and D. L. Baillie, 1994 The *Caenorhabditis elegans unc-60* gene encodes proteins homologous to a family of actin-binding proteins. Mol. Gen. Genet. **242:** 346–357.

Mello, C., and A. Fire, 1995 DNA transformation. Methods Cell Biol. **48:** 451–482.

Mello, C. C., J. M. Kramer, D. Stinchcomb and V. Ambros, 1991 Efficient gene transfer in *C.elegans*: extrachromosomal maintenance and integration of transforming sequences. EMBO J. **10:** 3959–3970.

Mukherjee, S., R. N. Ghosh and F. R. Maxfield, 1997 Endocytosis. Physiol. Rev. **77:** 759–803.

Munn, A. L., and H. Riezman, 1994 Endocytosis is required for the growth of vacuolar H(+)-ATPase-defective yeast: identification of six new END genes. J. Cell Biol. **127:** 373–386.

Nehrke, K., T. Begenisich, J. Pilato and J. E. Melvin, 2000 Into ion channel and transporter function. *Caenorhabditis elegans* ClC-type chloride channels: novel variants and functional expression. Am. J. Physiol. Cell Physiol. **279:** C2052–C2066.

Nonet, M. L., K. Grundahl, B. J. Meyer and J. B. Rand, 1993 Synaptic function is impaired but not eliminated in *C. elegans* mutants lacking synaptotagmin. Cell **73:** 1291–1305.

Nonet, M. L., A. M. Holgado, F. Brewer, C. J. Serpe, B. A. Norbeck *et al.*, 1999 UNC-11, a *Caenorhabditis elegans* AP180 homologue, regulates the size and protein composition of synaptic vesicles. Mol. Biol. Cell **10:** 2343–2360.

Otsuka, A. J., A. Jeyaprakash, J. Garcia-Anoveros, L. Z. Tang, G. Fisk *et al.*, 1991 The *C. elegans unc-104* gene encodes a putative kinesin heavy chain-like protein. Neuron **6:** 113–122.

Pancer, Z., J. P. Rast and E. H. Davidson, 1999 Origins of immunity: transcription factors and homologues of effector genes of the vertebrate immune system expressed in sea urchin coelomocytes. Immunogenetics **49:** 773–786.

Pearson, A. M., 1996 Scavenger receptors in innate immunity. Curr. Opin. Immunol. **8:** 20–28.

Qualmann, B., J. Roos, P. J. DiGregorio and R. B. Kelly, 1999 Syndapin I, a synaptic dynamin-binding protein that associates with the neural Wiskott-Aldrich syndrome protein. Mol. Biol. Cell **10:** 501–513.

Rappleye, C. A., A. R. Paredez, C. W. Smith, K. L. McDonald and R. V. Aroian, 1999 The coronin-like protein POD-1 is required for anterior-posterior axis formation and cellular architecture in the nematode *Caenorhabditis elegans*. Genes Dev. **13:** 2838–2851.

Reddien, P. W., and H. R. Horvitz, 2000 CED-2/CrkII and CED-10/Rac control phagocytosis and cell migration in *Caenorhabditis elegans*. Nat. Cell Biol. **2:** 131–136.

Richmond, J. E., W. S. Davis and E. M. Jorgensen, 1999 UNC-13 is required for synaptic vesicle fusion in *C. elegans*. Nat. Neurosci. **2:** 959–964.

Riddle, D. L., T. Blumenthal, B. J. Meyer and J. R. Priess, 1997 *C. elegans II*. Cold Spring Harbor Laboratory Press, Plainview, NY.

Riezman, H., 1985 Endocytosis in yeast: several of the yeast secretory mutants are defective in endocytosis. Cell **40:** 1001–1009.

Robbins, A. R., S. S. Peng and J. L. Marshall, 1983 Mutant Chinese hamster ovary cells pleiotropically defective in receptor-mediated endocytosis. J. Cell Biol. **96:** 1064–1071.

Robinson, M. S., C. Watts and M. Zerial, 1996 Membrane dynamics in endocytosis. Cell **84:** 13–21.

Saifee, O., L. Wei and M. L. Nonet, 1998 The *Caenorhabditis elegans*

unc-64 locus encodes a syntaxin that interacts genetically with synaptobrevin. Mol. Biol. Cell **9:** 1235–1252.

Sambrook, J., E. F. Fritsch and T. Maniatis, 1989 *Molecular Cloning: A Laboratory Manual*. Cold Spring Harbor Laboratory Press, Cold Spring Harbor, NY.

Seki, N., M. Muramatsu, S. Sugano, Y. Suzuki, A. Nakagawara *et al.*, 1998 Cloning, expression analysis, and chromosomal localization of HIP1R, an isolog of huntingtin interacting protein (HIP1). J. Hum. Genet. **43:** 268–271.

Sever, S., H. Damke and S. L. Schmid, 2000 Dynamin: GTP controls the formation of constricted coated pits, the rate limiting step in clathrin-mediated endocytosis. J. Cell Biol. **150:** 1137–1148.

Shibata, Y., T. Fujii, J. A. Dent, H. Fujisawa and S. Takagi, 2000 EAT-20, a novel transmembrane protein with EGF motifs, is required for efficient feeding in *Caenorhabditis elegans*. Genetics **154:** 635–646.

Simpson, F., A. A. Peden, L. Christopoulou and M. S. Robinson, 1997 Characterization of the adaptor-related protein complex, AP-3. J. Cell Biol. **137:** 835–845.

Singleton, D. R., T. T. Wu and J. D. Castle, 1997 Three mammalian SCAMPs (secretory carrier membrane proteins) are highly related products of distinct genes having similar subcellular distributions. J. Cell Sci. **110:** 2099–2107.

Stack, J. H., and S. D. Emr, 1994 Vps34p required for yeast vacuolar protein sorting is a multiple specificity kinase that exhibits both protein kinase and phosphatidylinositol-specific PI 3-kinase activities. J. Biol. Chem. **269:** 31552–31562.

Steeg, P. S., G. Bevilacqua, L. Kopper, U. P. Thorgeirsson, J. E. Talmadge *et al.*, 1988 Evidence for a novel gene associated with low tumor metastatic potential. J. Natl. Cancer Inst. **80:** 200–204.

Steven, R., T. J. Kubiseski, H. Zheng, S. Kulkarni, J. Mancillas *et al.*, 1998 UNC-73 activates the Rac GTPase and is required for cell and growth cone migrations in *C. elegans*. Cell **92:** 785–795.

Sun, M., E. Goldin, S. Stahl, J. L. Falardeau, J. C. Kennedy *et al.*, 2000 Mucolipidosis Type IV is caused by mutations in a gene encoding a novel transient receptor potential channel. Hum. Mol. Genet. **9:** 2471–2478.

Swan, K. A., A. F. Severson, J. C. Carter, P. R. Martin, H. Schnabel *et al.*, 1998 *cyk-1*: a *C. elegans* FH gene required for a late step in embryonic cytokinesis. J. Cell Sci. **111:** 2017–2027.

Tabara, H., A. Grishok and C. C. Mello, 1998 RNAi in *C. elegans*: soaking in the genome sequence. Science **282:** 430–431.

Tan, M. W., and F. M. Ausubel, 2000 *Caenorhabditis elegans*: a model genetic host to study *Pseudomonas aeruginosa* pathogenesis. Curr. Opin. Microbiol. **3:** 29–34.

Tang, Z., T. Okamoto, P. Boontrakulpoontawee, T. Katada, A. J. Otsuka *et al.*, 1997 Identification, sequence, and expression of an invertebrate caveolin gene family from the nematode *Caenorhabditis elegans*. Implications for the molecular evolution of mammalian caveolin genes. J. Biol. Chem. **272:** 2437–2445.

Tcherepanova, I., L. Bhattacharyya, C. S. Rubin and J. H. Freedman, 2000 Aspartic proteases from the nematode *Caenorhabditis elegans*. Structural organization and developmental and cell-specific expression of asp-1. J. Biol. Chem. **275:** 26359–26369.

TerBush, D. R., T. Maurice, D. Roth and P. Novick, 1996 The exocyst is a multiprotein complex required for exocytosis in *Saccharomyces cerevisiae*. EMBO J. **15:** 6483–6494.

Timmons, L., and A. Fire, 1998 Specific interference by ingested dsRNA. Nature **395:** 854.

Venter, J. C., M. D. Adams, E. W. Myers, P. W. Li, R. J. Mural *et al.*, 2001 The sequence of the human genome. Science **291:** 1304–1351.

Wang, S. S., O. Devuyst, P. J. Courtoy, X. T. Wang, H. Wang *et al.*, 2000 Mice lacking renal chloride channel, CLC-5, are a model for Dent's disease, a nephrolithiasis disorder associated with defective receptor-mediated endocytosis. Hum. Mol. Genet. **9:** 2937–2945.

Watts, C., and M. Marsh, 1992 Endocytosis: What goes in and how? J. Cell Sci. **103:** 1–8.

Wendland, B., J. M. McCaffery, Q. Xiao and S. D. Emr, 1996 A novel fluorescence-activated cell sorter-based screen for yeast endocytosis mutants identifies a yeast homologue of mammalian eps15. J. Cell Biol. **135:** 1485–1500.

White, J., 1988 The anatomy, pp. 81–122 in *The Nematode Caenorhabditis elegans*, edited by W. Wood. Cold Spring Harbor Laboratory Press, Cold Spring Harbor, New York.

Williams, B. D., B. Schrank, C. Huynh, R. Shownkeen and R. H. Waterston, 1992 A genetic mapping system in *Caenorhabditis elegans* based on polymorphic sequence-tagged sites. Genetics **131:** 609–624.

Wu, Y. C., and H. R. Horvitz, 1998 *C. elegans* phagocytosis and cell-migration protein CED-5 is similar to human DOCK180. Nature **392:** 501–504.

Yeung, B. G., H. L. Phan and G. S. Payne, 1999 Adaptor complex-independent clathrin function in yeast. Mol. Biol. Cell **10:** 3643–3659.

Zhang, Y., B. Grant and D. Hirsh, 2001 RME-8, a conserved J-domain protein, is required in endocytosis in *C. elegans*. Mol. Biol. Cell **12:** 2011–2021.

Zheng, B., J. N. Wu, W. Schober, D. E. Lewis and T. Vida, 1998 Isolation of yeast mutants defective for localization of vacuolar vital dyes. Proc. Natl. Acad. Sci. USA **95:** 11721–11726.

Zipkin, I. D., R. M. Kindt and C. J. Kenyon, 1997 Role of a new Rho family member in cell migration and axon guidance in *C. elegans*. Cell **90:** 883–894.

Communicating editor: B. J. Meyer